

Validation of reactivity descriptors to assess the aromatic stacking within the tyrosine gate of FimH

Goedele Roos^{1,2,3,*}, Adinda Wellens², Mohamed Touaibia^{4,5}, Paul Geerlings¹, René Roy⁴, Lode Wyns², Julie Bouckaert^{2,6,*}

¹General Chemistry, Vrije Universiteit Brussel, 1050 Brussels, Belgium

²Structural Biology Brussels, VIB and Vrije Universiteit Brussel, Pleinlaan 2, 1050 Brussels, Belgium

³Brussels Center for Redox Biology, 1050 Brussels, Belgium

⁴Department of Chemistry, Université du Québec à Montréal, Montréal, Qc, Canada H3C 3P8

⁵Present addresses: (MT): Department of Chemistry and Biochemistry, Université de Moncton, New Brunswick, Canada E1A 3E9

⁶Unité de Glycobiologie Structurale et Fonctionnelle), UMR8576 du CNRS, Université Lille 1, 59655 Villeneuve d'Ascq, France.

*Corresponding authors: groos@vub.ac.be, julie.bouckaert@univ-lille1.fr

Supplementary

Crystallization-data collection-structure determination

The FimH lectin domain (Phe1-Thr158 of the *fimH* gene product of *E. coli* strain J96) was expressed and purified as described.¹ The mannopyranosides series were synthesized as described.² Co-crystallizations of 16 and 12 mg/ml FimH concentration, respectively with inhibitors **1OMe** and **2OH** (see **Table 1** for the identification of the ligands) present in a 2 times molar excess, were set up by mixing equal volumes of the complex and the precipitant in sitting drops and using the vapor diffusion crystallization method. The precipitant was 1M NH₄COOH for FimH – **1OMe** and 70% 2-methyl-2,4-pentanediol for FimH – **2OH**. After one week equilibration at 293K, small needle-like crystals (~ 10 x 10 x 500 Å³) appeared. The crystals were flash-cooled at 100K in the precipitant solution complemented with 20% glycerol as cryoprotectant before data collection at 100K at the beamline Proxima1 at the SOLEIL synchrotron. The crystals diffracted to almost atomic resolution (**Table S1**). Spatial resolutions of 1.33 Å and of 1.60 Å for respectively FimH – **1OMe** and FimH – **2OH** were observed. The crystal data were indexed, processed and scaled using the XDS package.³ Initial phases were obtained by molecular replacement with the program PHASER⁴ using a monomer of FimH lectin domain (chain A of PDB entry 2VCO) as a search model. The resulting molecular replacement solution was submitted to restrained refinement using Refmac 5.2.0005,⁵ with 5% of the data retained for cross-validation purposes. Several cycles of successive maximum likelihood restrained refinement using Refmac 5.2.0005 were combined with manual model adjustment and electron density inspection performed in COOT

graphics.⁶ Geometric restraints for compounds **1OMe** and **2OH** were generated by elbow from the Phenix suite.⁷ The solution of the molecular replacement contained one FimH lectin domain complex per asymmetric unit in the orthorhombic P 2₁ 2₁ 2₁ space group. The ligand was clearly defined in the electron density in both crystal structures (**Figures 1C** and **E**). Pictures were prepared with Pymol version 0.99.

1. Wellens, A., Garofalo, C., Nguyen, H., Van Gerven, N., Slattegard, R., Hernalsteens, J. P., Wyns, L., Oscarson, S., De Greve, H., Hultgren, S., and Bouckaert, J. (2008) Intervening with urinary tract infections using anti-adhesives based on the crystal structure of the FimH-oligomannose-3 complex. *PLoS ONE*. 3, e2040.
2. Touaibia, M., Wellens, A., Glinschert, A., Shiao, T. C., Wang, Q., Papadopoulos, A., Bouckaert, J., and Roy, R. (2013) O- and C-linked mannopyranosides to chemically disarm uropathogenic *Escherichia coli* by targeting their type-1 fimbriae mediated adhesion. *To be published*.
3. Kabsch, W. (1993) Automatic processing of rotation diffraction data from crystals of initially unknown symmetry and cell constants. *J. Appl. Crystallogr.* 26, 795-800.
4. McCoy, A. J. (2007) Solving structures of protein complexes by molecular replacement with Phaser. *Acta Crystallogr. , Sect. D: Biol. Crystallogr.* 63, 32-41.
5. Murshudov, G. N., Vagin, A. A., and Dodson, E. J. (1997) Refinement of macromolecular structures by the maximum-likelihood method. *Acta Crystallogr. , Sect. D: Biol. Crystallogr.* 53, 240-255.
6. Emsley, P. and Cowtan, K. (2004) Coot: model-building tools for molecular graphics. *Acta Crystallogr. , Sect. D: Biol. Crystallogr.* 60, 2126-2132.
7. Moriarty, N. W., Grosse-Kunstleve, R. W., and Adams, P. D. (2009) electronic Ligand Builder and Optimization Workbench (eLBOW): a tool for ligand coordinate and restraint generation. *Acta Crystallogr. D. Biol. Crystallogr.* 65, 1074-1080.

Calculation details of E_{int} and E_{disp}

To gain insight in the measured affinities, interaction energies between various ligands and the tyrosines 137 and 48 were calculated starting from the X-ray structures at the MP2/6-311++G(d,p) level in gas phase using basis set superposition error correction via the counterpoise method (**Table 1**). Prior to interaction energy calculations, hydrogen atoms were placed and optimized at the B3LYP/6-311++G(d,p) level. The dispersion part of the interaction energy was calculated by subtracting the Hartree-Fock interaction energy from the MP2 interaction energy ($E_{\text{int, disp}} = E_{\text{int, total}} - E_{\text{int, HF}}$). All calculations were performed using Gaussian03.¹

1. Frisch, M. J., Trucks, G. W., Schlegel, H. B., Scuseria, G. E., Robb, M. A., Cheeseman, J. R., Montgomery, Jr. A. J., Vreven, T., Kudin, K. N., Burant, J. C., Millam, J. M., Iyengar, S. S., Tomasi, J., Barone, V., Mennucci, B., Cossi, M., Scalmani, G., Rega, N., Petersson, G. A., Nakatsuji, H., Hada, M., Ehara, M., Toyota, K., Fukuda, R., Hasegawa, J., Ishida, M., Nakajima, T., Honda, Y., Kitao, O., Nakai, H., Klene, M., Li, X., Knox, J. E., Hratchian, H. P., Cross, J. B., Bakken, V., Adamo, C., Jaramillo, J., Gomperts, R., Stratmann, R. E., Yazyev, O., Austin, A. J., Cammi, R., Pomelli, C., Ochterski, J. W., Ayala, P. Y., Morokuma, K., Voth, G. A., Salvador, P., Dannenberg, J. J., Zakrzewski, V. G., Dapprich, S., Daniels, A. D., Strain, M. C., Farkas, O., Malick, D. K., Rabuck, A. D., Raghavachari, K., Foreman, J. B., Ortiz, J. V., Cui, Q., Baboul, A. G., Clifford, S., Cioslowski, J., Stefanov, B. B., Liu, G., Liashenko, A., Piskorz, P., Komaromi, I., Martin, R. L., Fox, D. J., Keith, T., Al-Laham, M. A., Peng, C. Y., Nanayakkara, A., Challacombe, M., Gill, P. M. W., Johnson, B., Chen, W., Wong, M. W., Gonzalez, C., and Pople, J. A. Gaussian 03, Revision A.1. 2003. Pittsburgh, PA.

Ref Type: Computer Program

Calculation of local hardness

The hardness and polarizability are calculated on the reference systems benzene and ethyne and on compounds **1OMe** and **2OH** and their respective hydroxyl (**1OH**) and methoxy (**2OMe**) derivatives, and on ligand **3**, **HM** and **BM** (**Table 2**). The components are modeled without the mannose (**Figure S1**) and optimized with Gaussian03¹ at the B3LYP/6-311+G(d,p) level. A frequency calculation was performed to ensure a local minimum. The local hardness $\eta(r)$ is calculated as the electronic part of the molecular electrostatic potential divided by two times the number of electrons:^{2,3}

$$\eta(r) = -\frac{V_{el}(r)}{2N}$$

with N the numbers of electrons and V_{el} the electronic part of the molecular electrostatic potential, given by:

$$-\int \frac{\rho(r')}{|r-r'|} dr'$$

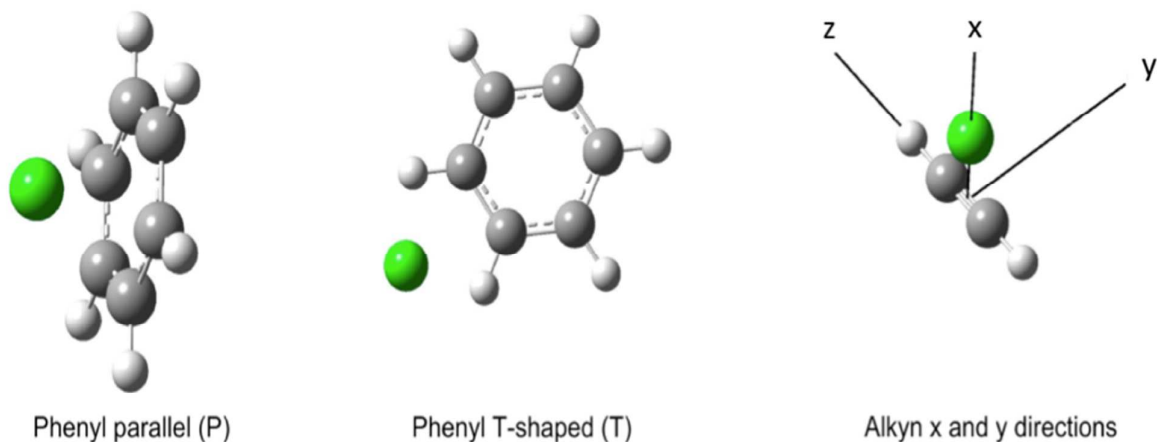
ρ is the electron density within a sphere with radius r .

1. Frisch, M. J., Trucks, G. W., Schlegel, H. B., Scuseria, G. E., Robb, M. A., Cheeseman, J. R., Montgomery, Jr. A. J., Vreven, T., Kudin, K. N., Burant, J. C., Millam, J. M., Iyengar, S. S., Tomasi, J., Barone, V., Mennucci, B., Cossi, M., Scalmani, G., Rega, N., Petersson, G. A., Nakatsuji, H., Hada, M., Ehara, M., Toyota, K., Fukuda, R., Hasegawa, J., Ishida, M., Nakajima, T., Honda, Y., Kitao, O., Nakai, H., Klene, M., Li, X., Knox, J. E., Hratchian, H. P., Cross, J. B., Bakken, V., Adamo, C., Jaramillo, J., Gomperts, R., Stratmann, R. E., Yazyev, O., Austin, A. J., Cammi, R., Pomelli, C., Ochterski, J. W., Ayala, P. Y., Morokuma, K., Voth, G. A., Salvador, P., Dannenberg, J. J., Zakrzewski, V. G., Dapprich, S., Daniels, A. D., Strain, M. C., Farkas, O., Malick, D. K., Rabuck, A. D., Raghavachari, K., Foreman, J. B., Ortiz, J. V., Cui, Q., Baboul, A. G., Clifford, S., Cioslowski, J., Stefanov, B. B., Liu, G., Liashenko, A., Piskorz, P., Komaromi, I., Martin, R. L., Fox, D. J., Keith, T., Al-Laham, M. A., Peng, C. Y., Nanayakkara, A., Challacombe, M., Gill, P. M. W., Johnson, B., Chen, W., Wong, M. W., Gonzalez, C., and Pople, J. A. Gaussian 03, Revision A.1. 2003. Pittsburgh, PA.

Ref Type: Computer Program

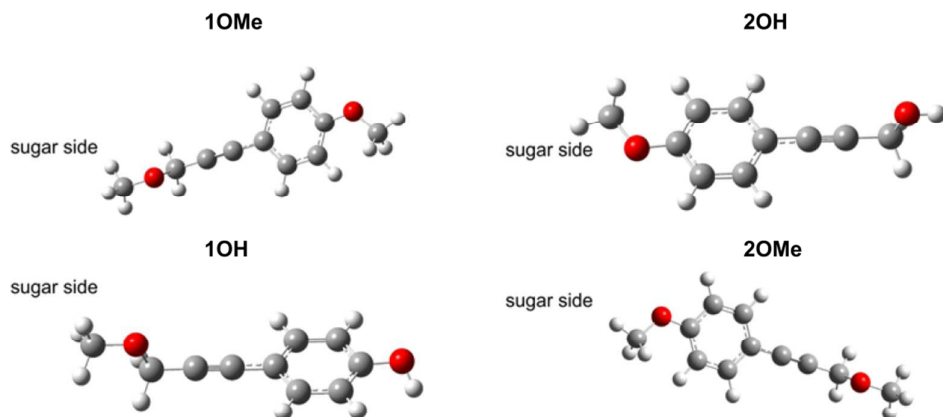
2. Mignon, P., Loverix, S., Steyaert, J., and Geerlings, P. (2005) Influence of the pi-pi interaction on the hydrogen bonding capacity of stacked DNA/RNA bases. *Nucleic Acids Res.* 33, 1779-1789.

3. Bercowitz, M. and Parr, R. G. (1985) On the concept of local hardness in chemistry. *J Am. Chem Soc.* 107, 6811.

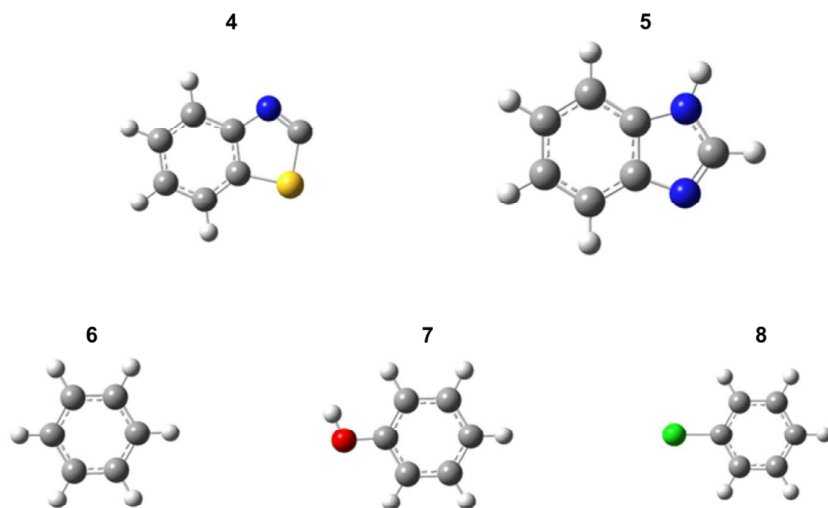


Supplementary Figure S1. The local hardness is evaluated at 1.7 Å above (parallel position) or sideward (T-shaped position) of the benzene rings¹. For the ethyn group, the local hardness is calculated at 1.7 Å in the x and y direction with respect to the triple bond in the z-direction.

1. Mignon, P., Loverix, S., Steyaert, J., and Geerlings, P. (2005) Influence of the pi-pi interaction on the hydrogen bonding capacity of stacked DNA/RNA bases. *Nucleic Acids Res.* 33, 1779-1789.



Supplementary Figure S2. Minimal structures used for calculation of polarizability and local hardness. Color code: gray: carbon, white: hydrogen, red: oxygen.



Supplementary Figure S3. Minimal structures used for calculation of polarizability and local hardness. Color code: gray: carbon, white: hydrogen, red: oxygen, blue: nitrogen, green: fluor.

Supplementary Table S1: Crystal data collection and processing, crystal parameters and refinement.

	FimH – 1OMe	FimH – 2OH
Data collection		
X-ray wavelength (Å)	0.918	0.980
Resolution range (Å)	48.17 - 1.25	31.78 - 1.53
Highest resolution shell (Å)	1.40 - 1.25	1.60 - 1.53
Space group	P2 ₁ 2 ₁ 2 ₁	P2 ₁ 2 ₁ 2 ₁
Unit cell dimensions		
<i>a</i> (Å)	31.01	32.92
<i>b</i> (Å)	42.30	42.29
<i>c</i> (Å)	96.35	96.34
Crystal mosaicity	0.19	0.40
R _{merge} (%) ^b	6.2 (42.0)	6.4 (34.7)
R _{meas} (%) ^c	7.1 (32.1)	6.8 (37.0)
I/σ _I	17.9 (4.2)	22.9 (4.3)
Completeness (%)	93.46 (86.0)	99.8 (98.8)
Redundancy	4.3 (3.2)	8.1 (7.6)
Wilson B-factor (Å ²)	12.7	20.3
Refinement		
R _{work}	14.98	16.04
R _{free}	17.75	18.52
Average B-factor	4.5	12.2
Root mean square deviation		
Bonds (Å)	0.006	0.007
Angles (°)	1.242	1.245
Residues in allowed regions		
(%) of Ramachandran plot	100.00	99.30
PDB entry code	4att	4auj

^aValues in parentheses indicate statistics for the highest resolution shell

^bR_{merge} = $\sum_h \sum_i |I_{h,i} - \langle I_h \rangle| / \sum_h \sum_i I_{h,i}$, where $I_{h,i}$ is the i^{th} observation of reflection h and $\langle I_h \rangle$ is the weighted average intensity for all observations i of reflection h

^cR_{meas} = redundancy-independent R-factor of equivalent reflections (intensities)¹⁰